

# On-sky SiPM Performance Measurements for Millisecond to Sub-Microsecond Optical Source Variability Studies

Albert Wai Kit Lau<sup>a,\*</sup>, Mehdi Shafiee<sup>b</sup>, George F. Smoot<sup>b,c,d,e</sup>, Bruce Grossan<sup>b,d</sup>, Siyang Li<sup>f</sup>, Zhanat Maksut<sup>b</sup>

<sup>a</sup>Department of Physics, The Hong Kong University of Science and Technology

<sup>b</sup>Energetic Cosmos Laboratory, Nazarbayev University, Kazakhstan

<sup>c</sup>Director of Centre for Fundamental Physics, IAS TT and WF Chao Professor, Institute for Advanced Study, Hong Kong University of Science and Technology

<sup>d</sup>Lawrence Berkeley National Laboratory, University of California, Berkeley

<sup>e</sup>Universit Sorbonne Paris Cit, Laboratoire APC-PCCP, Universit Paris Diderot

<sup>f</sup>Department of Physics, University of California, Berkeley, USA

**Abstract.** As part of our "Ultra-Fast Astronomy" (UFA) program, we present initial measurements of silicon photomultiplier detector (SiPM) performance for application to measurement of variability of optical astronomical targets on millisecond and shorter time scales. We mounted two different SiPM detectors at the focal plane of the 0.7 meter Nazarbayev University Transient Telescope at the Assy-Turgen Astrophysical Observatory (NUTTeA-TAO), with no filter in front of the detector, and measured their performance. The  $3\text{mm} \times 3\text{mm}$  SiPM detectors had a field of view of  $2.2716' \times 2.2716'$  for each SiPM channel. During the nights of 28-29/10/2019, we measured sky background, bright stars, and an artificial source with a 100Hz flashing frequency. We compared detected SiPM counts with Gaia satellite G band flux values to show that our SiPM detectors have linear response. With our two SiPMs (models S14520-3050VS and S14160-3050HS), we measured a dark current of  $\sim 130$  and  $\sim 85$  kilo count per second (kcps), and a sky background of  $\sim 191$  and  $\sim 203$  kcps, respectively. We measured an intrinsic crosstalk of 10.34% and 10.52% for the two detectors, respectively. We derive a  $5\sigma$  sensitivity of 14.7 and 15.2 Gaia G-band magnitude for 200ms exposures, for the two detectors, respectively. We derive, for transient events in  $10\mu\text{s}$  time window, a sensitivity of 20 detected photons or 6.1 Gaia G-band magnitudes. For shorter timescales, e.g. 100ns, our detection limit is limited by crosstalk to 12 detected photons, which correspond to fluence of  $\sim 133$  photons per square meter within 100ns.

**Keywords:** Silicon photomultiplier, Ultra Fast Astronomy, Optical Variability, Millisecond.

\*Albert Wai Kit Lau, [awklau@connect.ust.hk](mailto:awklau@connect.ust.hk)

## 1 Introduction

In our "Ultra Fast Astronomy" (UFA) program, we are aiming to survey the sky at sub-second (ns to ms) time scale.<sup>1</sup> It seems reasonable to search for variability on these time scales among the fastest-known sources of variability and transients (e.g. X-ray binaries and pulsars). Fast radio bursts (FRBs) are observed to have millisecond variations in the radio; these could be intrinsically orders of magnitude faster if there were accompanying emission in the optical.<sup>2</sup> Arguments have

been made that optical bands are favorable for interstellar communication due to high bandwidth, and so short time scales would be necessary for optical SETI.<sup>3</sup>

The primary goals of UFA project includes optical observation to millisecond pulsars and search of optical counterparts with FRBs detection. The search for these sub-second transient events using traditional CCD-like cameras is limited by readout noise and frame rate. Non-integrating photon detectors like a Photomultiplier Tube (PMT) or a Silicon Photomultiplier (SiPM) are necessary for exploring these ultra-fast time scales.

Recently, we began initial measurements of the sky using a SiPM-based testing camera on the 0.7-m aperture Nazarbayev University Transient Telescope at the Assy-Turgen Astrophysical Observatory (NUTTeIA-TAO).<sup>4</sup> This experiment serve as our first on-sky calibration test of SiPM and verify the possibility of SiPM as Ultra Fast Astronomy detector. In the experiment, two different models of SiPM were used to measure sky background, bright stars and an artificial millisecond period source. The experiment was performed at night of 28 and 29, October 2019 with environment temperature roughly 0°C and sky ambient temperature in range of  $-25^{\circ}\text{C}$  to  $-30^{\circ}\text{C}$ , which indicates a slightly cloudy sky.

In this paper we present our experimental setup, observation log, data processing. The data was compared with the standard G-band flux data from the Gaia satellite archive for analysis.<sup>5,6</sup> Calculation of detection lower limits at different time scales and noise including SiPM crosstalk, dark count and sky background are also presented. Finally, we proposed some necessary improvements to the detector for future observations.

## 2 Experimental setup

Figure 1 shows the whole setup for this experiment at Assy-Turgen astrophysical observatory. As it is shown on the right port of telescope is occupied by our detectors for UFA project.

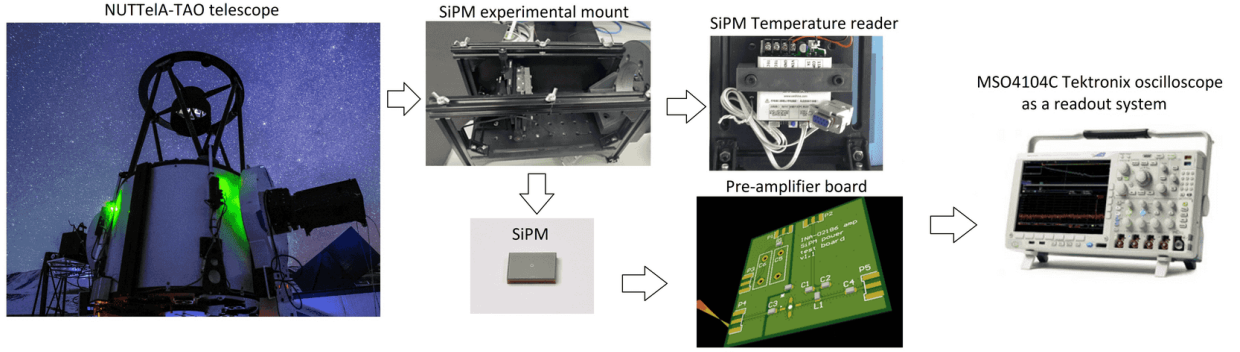


Fig 1: Experimental Setup for UFA project. The left image shows the telescope on whose right side is the port on which the SiPM experiment is mounted. The center shows the SiPM mount, hardware and electronics and on the right an image of the oscilloscope used to take the observations.

### 2.1 SiPM and Readout System

#### 2.1.1 SiPM

SiPM is a relatively recent technology which provides single photon resolving ability on a solid state chip. SiPM achieve the single and multiple photon resolving power by massive parallel geiger mode avalanche diodes (Micropixels) which produce a constant photon gain<sup>7</sup> of  $10^6$ . SiPM has high immunity to excess light exposure, much lower working voltage and higher overall quantum efficiency compared to PMT, but with the trade off of higher crosstalk and dark count noise. In this experiment, We used single channel SiPM models S14160-3050HS and S14520-3050VS from Hamamatsu.<sup>8</sup> The specifications of these two models are given at table 1. (Standard condition at  $25^\circ\text{C}$ );

Dark count noise of SiPM significantly is reduced at lower temperature. During the experiment, we ran the SiPMs at  $\sim 0^\circ\text{C}$  by natural cooling. Since the breakdown voltage of SiPM

Table 1: Specification of the SiPMs

Specifications	SiPM s14160-3050HS	SiPM s14160-3050VS
photosensitive area per channel	$3.0\text{mm} \times 3.0\text{mm}$	$3.0\text{mm} \times 3.0\text{mm}$
Micropixel pitch	$50\mu\text{m}$	$50\mu\text{m}$
Per channel micropixel number	3531	3531
spectral response range	Appendix A Fig. 12	Appendix A Fig. 13
Peak sensitivity	50% @ 450nm	49% @ 450nm
Common breakdown voltage	38V	38V
Temperature coefficient of breakdown voltage	$34\text{mV/C}^\circ$	$34\text{mV/C}^\circ$
standard overvoltage	2.7V	3V
Common crosstalk probability	7%	5%
Common dark count	1Mcps	600kcps
Common photon gain	$2.5 \times 10^6$	$2.8 \times 10^6$

also decreases with decreasing temperature, we have made a breakdown voltage versus temperature measurement prior to the experiment at observatory (appendix B). The SiPM voltage is maintained all over the experiment at breakdown voltage plus standard over voltage. Standard over voltage in table 1 is provided by Hamamatsu (SiPM supplier): 2.7V for S14160-3050HS and 3V for S14520-3050VS .

### 2.1.2 pre-amplifier circuit

The signal of SiPM is in the form of a charge current pulse. We used a  $50\Omega$  shunt resistor to convert it into a voltage pulse, followed by a 30dB pre-amplifier ready for logging. The 30dB pre-amplifier is developed base on a Monolithic Microwave Integrated Circuit (MMIC) low noise amplifier INA02186.<sup>9</sup> The amplifier gives flat gain up to 1GHz with a simple circuit design. The SiPM is AC coupled to pre-amplifier with a single photon detected (1 p.e.) giving a  $\sim 5\text{mV}$  peak output.

### 2.1.3 data logging setup

In the experiment, a MSO4104C Tektronix oscilloscope was configured to act as a data logging system.<sup>10</sup> To simulate our proposed next-generation data logging scheme, we limited the sampling rate of the oscilloscope to  $100\text{M}sp\text{s}$  with bandwidth of  $20\text{MHz}$  which is similar to common ADC data acquisition systems. Due to the memory limitation of the oscilloscope, we could take  $10^7$  data points for each measurement, corresponding to 0.2s observation time on each target.

### 2.2 Telescope specification

The NUTTelA-TAO telescope is designed for measuring prompt emission of gamma ray bursts (GRBs) which is able to complete pointing less than 8 seconds (See Fig.1). The telescope of model CDK700 has two Nasmyth focus ports, with the one occupied by Burst Simultaneous Three-Channel Instrument (BSTI) project. For UFA experiments, we are using the second port. The specifications of telescope are given in table 2.<sup>4</sup>

Table 2: Specification of telescope NUTTelA-TAO (CDK700)

diameter of primary mirror	0.7m
Central Obstruction	47% Primary Mirror Diameter
Focal length	4540mm (F6.5)
Effective light collection area	$2.998\text{m}^2$
Optimal field of view	70mm ( $0.86^\circ$ )
Image Scale	$22\mu\text{m}$ per arcsecond

By coupling the  $3\text{mm}\times 3\text{mm}$  SiPM onto NUTTelA-TAO with prime focus, we are obtained  $2.2716'\times 2.2716'$  viewing solid-angle on one SiPM channel. The light collection area was  $0.2998\text{m}^2$

## 3 Observation details

We performed measurements on two consecutive nights. The condition for experiments including list of observed targets beside weather conditions at each night are listed below:

### 3.1 S14160-3050HS observation: 28/10/2019

At first night of the test, the sky was slightly cloudy, humidity of 60% and sky ambient temperature of  $-25^{\circ}\text{C}$  as measured by our Boltwood Cloud Sensor II. Thus we chose a group of dimmer stars near zenith to minimize atmosphere effect. Observation were made with SiPM S14160-3050HS, with sensor temperature of  $-2.3^{\circ}\text{C}$  to  $-2.5^{\circ}\text{C}$ . Observation log is presented in Table 3.

Table 3: Observation log for 28/10/2019

Coordinate of pointing	Brightest star G-band magnitude	Time of observation	Airmass
RA 6h 51m 11.11s, DEC $58^{\circ} 25' 2.8''$	+7.93	04:24(+1d)	1.05
RA 6h 50m 54.42s, DEC $58^{\circ} 23' 5.7''$	+10.89	04:28(+1d)	1.04
RA 6h 56m 49.31s, DEC $58^{\circ} 21' 36.5''$	+13.11	04:32(+1d)	1.04
RA 6h 56m 40.19s, DEC $58^{\circ} 28' 53.4''$	+14.91	04:36(+1d)	1.04
RA 6h 56m 12.07s, DEC $58^{\circ} 39' 26.2''$	$>+18$	04:40(+1d)	1.04
dark count testing (shutter closed)	\	04:45(+1d)	\
RA 6h 53m 3s, DEC $59^{\circ} 26' 53.8''$	+5.2(saturation)	04:56(+1d)	1.04

### 3.2 S14520-3050VS observation: 29/10/2019

At second night of the test, we swapped the SiPM to S14520-3050VS. The sky was more clear with sky ambient temperature of  $-28^{\circ}\text{C}$  from Boltwood Cloud Sensor II. The sensor temperature was around  $2.4^{\circ}$  to  $2.6^{\circ}\text{C}$ . We repeated the measurement on same set of stars on previous day but with more airmass due to timing of the observations. Observation log is presented in table 4.

Table 4: Observation log for 29/10/2019

Coordinate of pointing	Brightest star G-band magnitude	Time of observation	Airmass
RA 6h 53m 3s, DEC $59^{\circ} 26' 53.8''$	+5.2(saturation)	23:17	1.71
RA 6h 51m 11.11s, DEC $58^{\circ} 25' 2.8''$	+7.93	23:21	1.66
RA 6h 50m 54.42s, DEC $58^{\circ} 23' 5.7''$	+10.89	23:24	1.64
RA 6h 56m 49.31s, DEC $58^{\circ} 21' 36.5''$	+13.11	23:27	1.66
RA 6h 56m 40.19s, DEC $58^{\circ} 28' 53.4''$	+14.91	23:31	1.64
RA 6h 56m 12.07s, DEC $58^{\circ} 39' 26.2''$	$>+18$	23:35	1.62
dark count testing (shutter closed)	\	23:39	\

## 4 Observation data processing

### 4.1 Noise reduction and baseline cancellation

Before measurements, we improved and calibrated the system to have less electrical and thermal noise. Main noise in our data comes from observatory power supply systems which has frequent unexpected voltage spikes with frequency of  $> 10\text{MHz}$ . By powering our pre-amplifier with this power source, our SiPM data were polluted with noise. We used a 21-point SavitzkyGolay low pass filter to get rid of this noise while we are preserving area under data pulse which has much lower frequency. The other parasitic source in our measured data is baseline which comes from AC to DC power converters and has low frequency of mainly  $< 100\text{Hz}$ . To cancel baseline, it is calculated from a 200 points moving mean filter with high pass cut-off frequency of  $500\text{kHz}$  then subtracted from the data.

The SiPM pulse has a sharp rise and a long decay tail of a few hundred ns. When multiple photons arrive within the signal recovery time, a pile up occurs. To calibrate this effect, the start point of each pulse is also calibrated to zero to ensure an accurate reading. Top-side of figure 2 shows part of dark count raw data which was measured by S14520-3050VS and bottom-side of same figure, shows processed data after noise reduction and baseline cancellation.

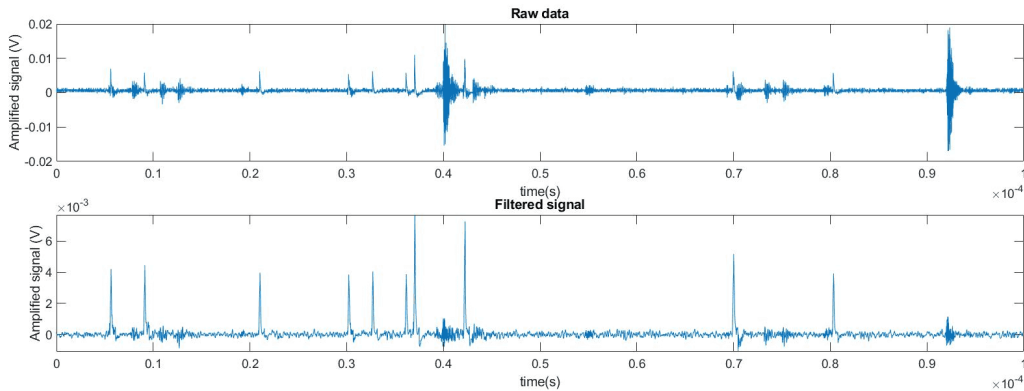


Fig 2: (Top) dark count raw data which was measured by S14520-3050VS, (bottom) processed data after filtration and baseline cancellation.

#### 4.2 Pulse area integration

As it is mentioned before, SiPM has a constant photon gain.<sup>7</sup> Therefore, the output charge ( $C = \int I dt$ ) indicate the number of arrival photons. In our shunt and pre-amplifier electronics, the charge is converted to a voltage pulse and the area under this pulse indicates the number of concurrently detected photons. Therefore, we perform a trapezoid integration of each voltage pulse to obtain its 'charge' (pulse area) and arrival time.

#### 4.3 SiPM P.E. peaks identification

After calculating the 'charge' (pulse area) of each pulse, we need to identify the number of arrival photons of the pulse. Ideally, a photon always gives the same amount of charge (constant gain<sup>7</sup>) and therefore the pulse area spectrum should be quantized (no half photon allowed in physics). In reality, the amount of calculated charge under each pulse can be effected by the electronic noise, pile-up effect leftover, variation in silicon sensor and readout system rounding error. As a result, the pulse area histogram plot becomes a Gaussian mixture: each quantized pulse area level spread into a Gaussian distribution. To reduce these parasitic effects and calculate the number of arrival photons, we implant a two-step Gaussian Mixture Model (GMM).<sup>11</sup>

1. We fit a 2-peaks GMM distribution to data using iterative Expectation-Maximization (EM) algorithm with starting guess generated from k-means++ algorithm which generate starting point of by nearest mean clustering.<sup>12,13</sup> This fitting provide us with the information of centroid (average peak area) and variance of first and second peaks (1 P.E. and 2 P.E.).
2. From centroid (average peak area) and variance of first and second peaks obtained in step 1, we estimate the centroid and variance of other P.E. peaks charge distribution using a linear



projection.

3. Having estimated values for centroid and variance of each P.E. peak we perform GMM fitting again to obtain the precise number of arrival photons.

Two-step GMM fitting is used since the first auto GMM fitting could not provide precise information about peaks of  $> 2$  P.E.

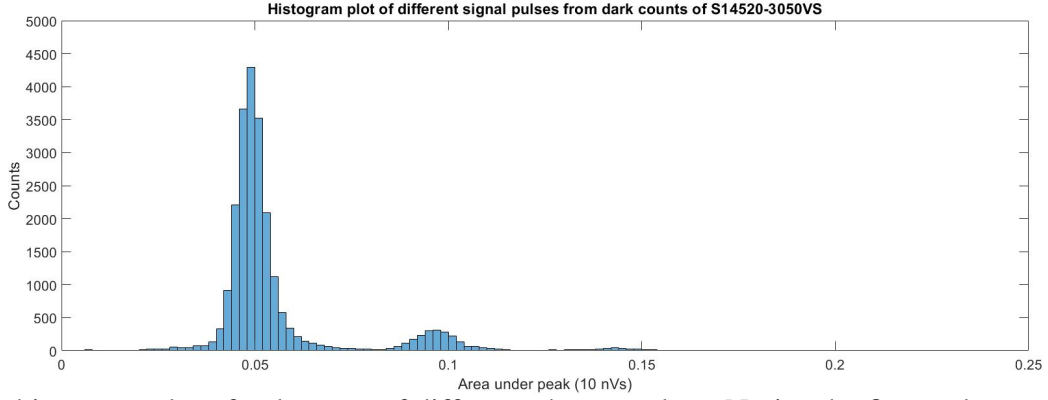


Fig 3: A histogram plot of pulse area of different photon pulses. Notice the first and second peaks are both Gaussian like and hence we use the Gaussian Mixture model for fitting.

#### 4.4 saturated data

In case of detecting bright stars by our SiPM, the SiPM output might pile up to a level that single pulse can not be distinguished any more which is called saturated. In this mode, SiPM can still accept more photons, but we can not identify them on photon counting basis. Figure 4 shows this case when we were observing 14 Lyn (a star with G-band +5.2 magnitude).

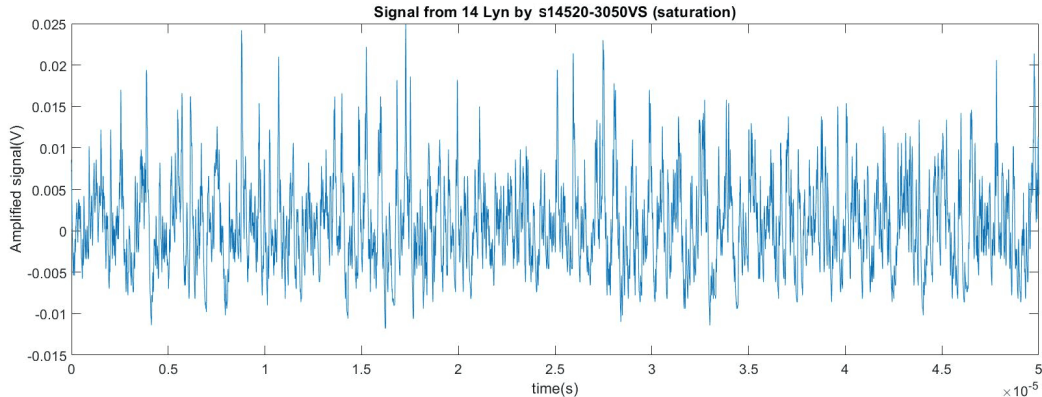


Fig 4: Part of data saturated by photon flux from 14 Lyn using SiPM S14520-3050VS.

From histogram plot, we can clearly see that GMM distribution for photon identification is disappeared (In simple word we cannot differentiate between 1 P.E. and 2 P.E. peaks anymore as it is shown in Fig.5 compare to Fig. 3)

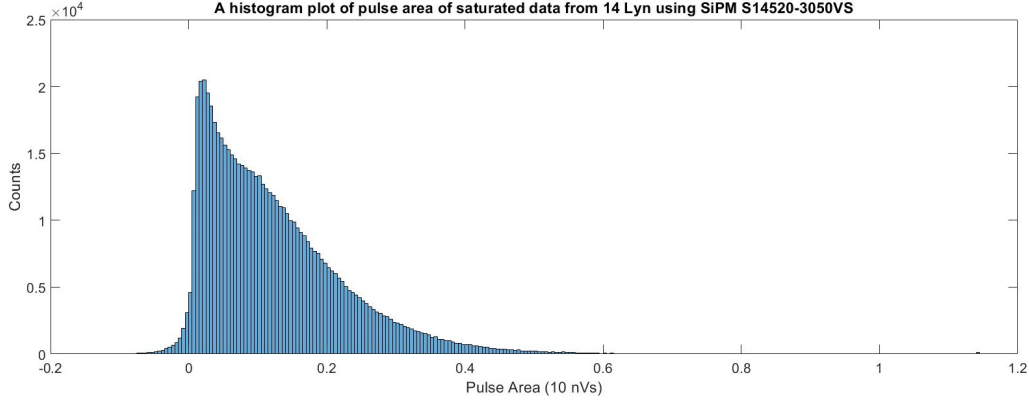


Fig 5: histogram plot from the above saturated data.

#### 4.5 crosstalk in SiPM

One severe noise affecting the observation from SiPM is the crosstalk which comes from both optics and electronics. When crosstalk happens, one photon input will produce a 2 or higher P.E. pulse which is indistinguishable from that real multiple P.E. signal.<sup>5</sup> The intrinsic crosstalk from SiPM is calculated as follow:

1. Measured crosstalk rate is calculated by equation 1.
2. Measured crosstalk rate is plotted versus recorded SiPM count
3. Using linear fitting to obtain the crosstalk at 0 SiPM count, which is the intrinsic crosstalk from SiPM.

Here we assume the photon rate is constant without bunching, so the number of multiple P.E. peaks ( $> 1$  P.E.) grow linearly with the detected photon rate. The equation for calculation of the measured crosstalk rate is:

$$\text{Measured crosstalk rate} = \text{intrinsic crosstalk} + \text{natural high P.E. rate} = \frac{> 1 \text{ p.e. SiPM count}}{\text{total SiPM count}} \quad (1)$$

## 5 Data Analysis

To verify the data, we compared our results with the standard G-band flux data from the Gaia satellite archive. Our SiPM has similar spectral response as Gaia G-band in the range of 400nm-900nm.<sup>5,6</sup> Since our SiPM does not have spatial resolution, therefore we cannot determine the orientation of detection field. Instead, we consider a circle with diameter of diagonal size of SiPM as our detection field (3.2125').

### 5.1 SiPM S14160-3050HS

In first night we used SiPM S14160-3050HS (See table 1, 3). We considered the airmass effects on photon flux calibration which is obtained by Gaia G-band satellite.<sup>14</sup> Table 5 shows calibrated flux, measured SiPM counts and calculated cross-talk rate (saturated data is not listed).

Table 5: Measured data from S14160-3050HS

Coordinate of pointing	calibrated flux (Gaia G-band)	SiPMs count in 200ms	cross-talk rate (%)
RA 6h 51m 11.11s, DEC 58° 25' 2.8"	12666833	341726	23.2
RA 6h 50m 54.42s, DEC 58° 23' 5.7"	894096	78615	13.61
RA 6h 56m 49.31s, DEC 58° 21' 36.5"	126519	63231	13.08
RA 6h 56m 40.19s, DEC 58° 28' 53.4"	29035	58415	12.82
RA 6h 56m 12.07s, DEC 58° 39' 26.2"	4128	53769	12.57
dark count testing (shutter closed)	\	16988	10.72

Figure 6 shows measured count rate versus calibrated G-band flux.

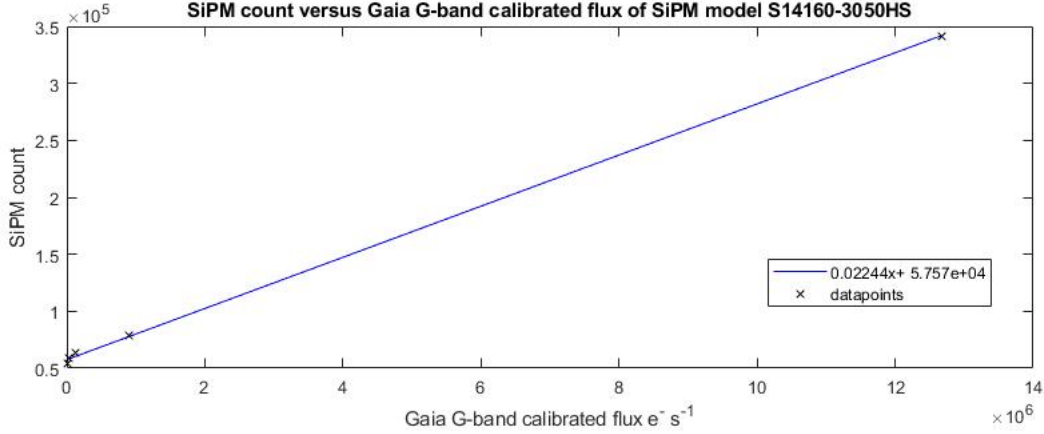


Fig 6: SiPM Count in 0.2s versus calibrated G-band flux for s14160-3050HS

From figure 6, SiPM dark count is  $\sim 85$  kilo count per second (kcps) while the sky background is  $\sim 203$ kcps after subtracting the dark count.

Also, consider the measurement at RA 6h 56m 40.19s, DEC  $58^\circ 28' 53.4''$  (calibrated Gaia G band flux  $29035 e^- s^{-1}$ ) versus RA 6h 56m 12.07s, DEC  $58^\circ 39' 26.2''$  (calibrated Gaia G band flux  $4128 e^- s^{-1}$ ): SiPM received 58415 counts with  $5\sigma$  range of  $\pm 1208$  from first source and 53769 counts with  $5\sigma$  range of  $\pm 1159$  counts from second source. Since the difference between two measurements is 4646 counts, it is clearly larger than the  $5\sigma$  range. Consider the different in gaia G band flux of two source of  $24907 e^- s^{-1}$ , it is equivalent to a point source of 14.7 mag of G band resolved in 200ms window.

Figure 7 shows the measured crosstalk versus count rate. Intrinsic crosstalk of SiPM S14160-3050HS is measured to be 10.52%.

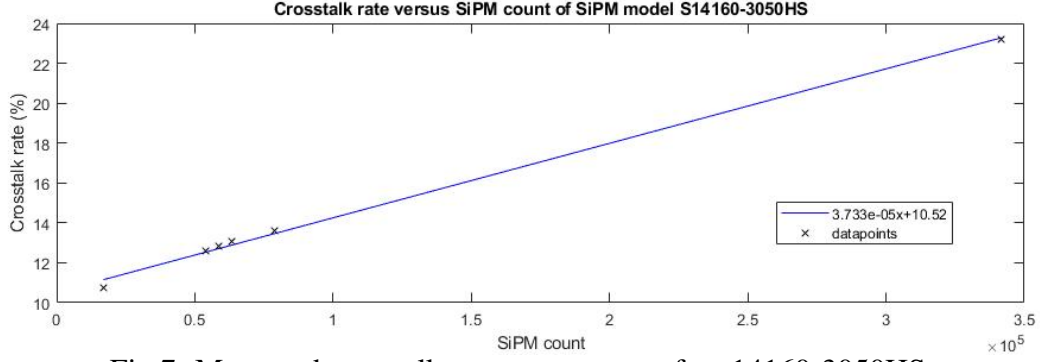


Fig 7: Measured crosstalk versus count rate for s14160-3050HS

## 5.2 SiPM S14520-3050VS

In second night we used SiPM S14520-3050VS (See table 1, 4). We did the same measurement as first night for G-band flux calibration, SiPM counts and measured cross-talk which are given in table 6.

Table 6: Measured data from S14520-3050VS

Coordinate of pointing	calibrated flux (Gaia G-band)	SiPMs count in 200ms	cross-talk rate (%)
RA 6h 51m 11.11s, DEC 58° 25' 2.8"	8545608	304481	23.34
RA 6h 50m 54.42s, DEC 58° 23' 5.7"	894096	82317	13.94
RA 6h 56m 49.31s, DEC 58° 21' 36.5"	79265	69858	13.27
RA 6h 56m 40.19s, DEC 58° 28' 53.4"	18412	67854	12.9
RA 6h 56m 12.07s, DEC 58° 39' 26.2"	2650	64171	13.11
dark count testing (shutter closed)	\	26103	11.65

Figure 8 shows SiPM count rate versus calibrated G-band flux.

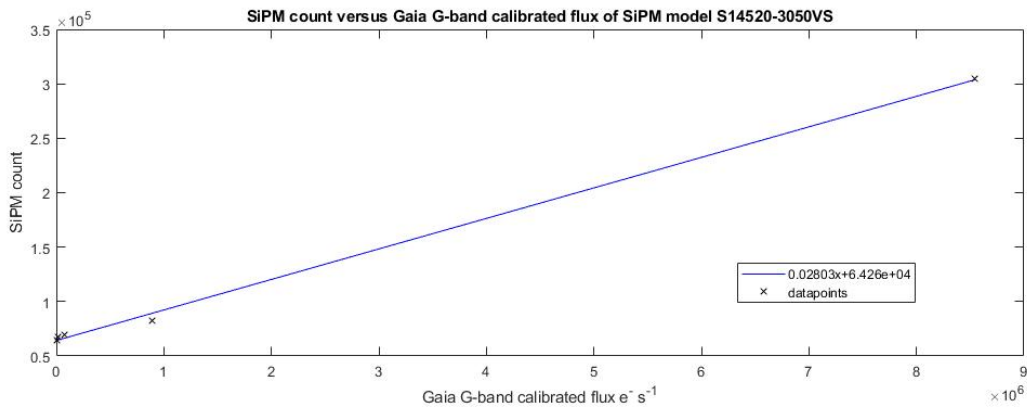


Fig 8: Count rate versus calibrated G-band flux for S14520-3050VS.

From figure 8, SiPM dark count is  $\sim 130\text{kps}$  while the sky background is  $\sim 191\text{kps}$  after subtracting the dark count.

Also, consider the measurement at RA 6h 56m 40.19s, DEC  $58^\circ 28' 53.4''$  (calibrated Gaia G band flux  $18412e^-s^{-1}$ ) versus RA 6h 56m 12.07s, DEC  $58^\circ 39' 26.2''$  (calibrated Gaia G band flux  $2650e^-s^{-1}$ ): SiPM received 67854 counts with  $5\sigma$  range of  $\pm 1302$  from first source and 64171 counts with  $5\sigma$  range of  $\pm 1267$  counts from second source. Since the difference between two measurements is 3683 counts, it is clearly larger than the  $5\sigma$  range. Consider the different in gaia G band flux of two source of  $15762e^-s^{-1}$ , it is equivalent to a point source of 15.2 mag of G band resolved in 200ms window.

Figure 9 shows the measured crosstalk versus count rate. Intrinsic crosstalk of SiPM S14520-3050VS is measured to be 10.34%.

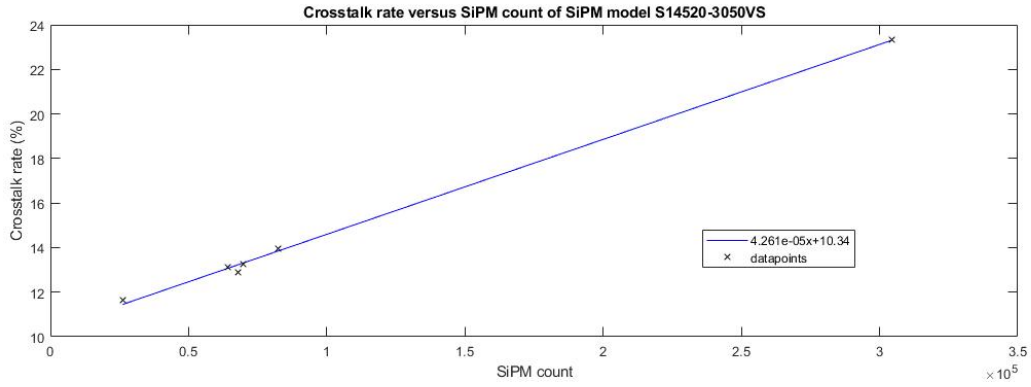


Fig 9: Measured crosstalk versus count rate for S14520-3050VS.

### 5.3 time domain analysis

The purpose of using SiPM on astrophysical detection is the ability of resolving fast events within several milli-seconds. During all observations of the stars, no significant change in brightness is measured as expected. We applied both  $10\mu s$  and  $1ms$  moving mean filtered on smoothed light

curves in all observations. These light curves, together with the histogram plot of photon statistics and corresponding Gaia star chart of observation are attached in the appendix C and D.

### 5.3.1 Synthetic light source test

To simulate the effect of fast transient signal on our detector, we diffused some synthetic  $\sim 100Hz$  square wave light to the SiPM at the middle of observation. We could see easily this light source in our measurements as it is shown in figure 10.

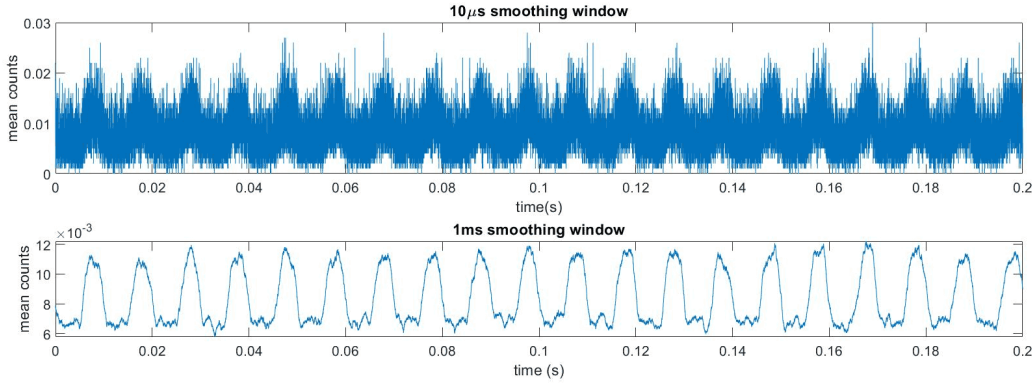


Fig 10:  $10\mu s$  (top) and  $1ms$  (bottom) smoothed signal from synthetic  $100Hz$  scattered square wave light.

In the figure 10,  $100Hz$  signal can be seen after using moving mean filters with  $10\mu s$  and  $1ms$  windows. Using  $1ms$  window gives much better SNR compared to  $10\mu s$ .

### 5.3.2 Sensitivity in different time bin

Since the Ultra Fast Astronomy (UFA) project is mainly aimed at detection of fast transients, we need to propagate detection limits of SiPMs under different time binning.

Consider a very dark portion of the sky, just like the area without star brighter than 18 mag in Gaia G band we chose in table 4 and 6. Using the SiPM S14520-3050VS, what is the minimum brightness of transient can we detect?

For fast transient, we need to consider Poisson statistic since photon comes one by one. Also we can no longer use the  $5\sigma$  criterion since a huge number of measurement is taken every second,  $5\sigma$  still give us a high false alarm rate. First, we fit the data to a Poisson distribution:

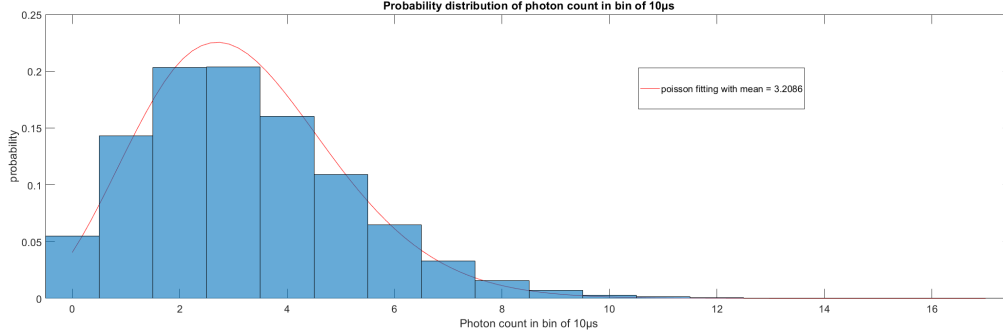


Fig 11: Poisson statistical fitting of SiPM measurement on a sample dark sky

From figure 11, we find that the mean photon income is 3.2086 per  $10\mu s$ . Assume our desired false alarm rate is less than 1 event per night ( $\sim 50000s$ ), we need a confidence threshold of 0.9999999998. From simple Poisson statistic, it correspond to a detection threshold of 20 photon detected within  $10\mu s$ . Comparing to above count rate versus calibrated G-band flux (figure 8), the transient should give G band flux at least  $69059579 e^- s^{-1}$  ( $\sim 6.1$  G-band mag) within  $10\mu s$ .

For detection of ns transient, the detection limit will be limited by crosstalk: consider event of 100ns, the average count will be 0.032086, and 1 false event per night limit require confidence threshold of 0.999999999998. This give us a limit of 5 photons received in 100ns. However, under crosstalk of 10%, 5 photons false alarm rate is  $0.1^5 = 0.00001$  which is far too high. To maintain the confidence threshold of 0.999999999998, we need at least 12 photons detected. Considering a average detection efficiency of  $\sim 30\%$  over 300nm to 900nm and collection area  $0.2998m^2$  of the NUTTeIA-TAO system, this convert to fluence of roughly 133 photons per square meter within 100ns.



## 6 Future improvements and plans

According to our experiments, we found out by using both models of SiPMs, our detection ability is limited between  $\sim 15$  magnitude to  $\sim 7$  magnitude (saturation). To perform astrophysical measurement for fast transient events, we expect to have higher sensitivity. Taking the Crab pulsar *PSRB0531 + 21* as a sample, the pulsar itself is 16.5 V-band magnitude embedded in a bright 8.4 V-band magnitude nebula.<sup>15</sup> Therefore, we should improve our detector to resolve a dim point source from a bright nearby background.

Currently, the SiPM sensitivity is mainly limited by the spatial resolution. In our experiment, the single channel detection field is  $2.2716' \times 2.2716'$  which is equivalent with  $18576.6 \text{ arcsecond}^2$ . In the experiment, sky background is measured to be around 200kcps for both models. Providing a sensor with higher spatial sensitivity can greatly reduce the effect of sky background. If the sensor can give  $10'' \times 10''$  spatial resolution, the equivalent sky noise will be reduced by 185 times, which is roughly 5.7 magnitude improvement. Same improvement can be achieved in dark count noise due to its scale with sensor area. Therefore, we aim to develop a SiPM based detector with better spatial resolution for next run.

In the experiment, both SiPMs have a higher intrinsic crosstalk compared to the common values given by hamamatsu (10.52% versus 7% for S14160-3050HS and 10.34% versus 5% for S14520-3050VS). Possible reasons includes a thin layer of frozen moisture on sensor surface or internal reflection from mounts and telescope mirrors.

For the readout system, an standalone FPGA system need to be developed for long term observation. We are planning to use a system-on-chip (SoC) FPGA with integrated ARM core to host a linux based system. The SiPM signal should be converted to digital data using high speed ADC

then logged by FPGA. The FPGA system can calculate the statistical significance of real time data. If any possible event is detected, the system should log the raw photon arrival information and fire an alarm to notice the astronomer.

During this experiment, we also observed strong noise from power supply. To remove the noise, we will develop an isolated power for both SiPM and the analog readout system.

## **7 Conclusion**

The initial measurements of silicon single photon detector for Ultra-Fast Astronomy is successfully performed on NUTTelA-TAO telescope. The  $3\text{mm} \times 3\text{mm}$  SiPM sensors both provide a detection limit of 14.7 G-band magnitude (S14160-3050HS) and 15.2 G-band magnitude (S14520-3050VS) in 200ms observation window. The sky background and intrinsic crosstalk were measured to be  $\sim 191, 203$  kcps and 10.34%, 10.52% for both S14160-3050HS and S14520-3050VS respectively. The  $10\mu\text{s}$  detection limit is propagated to be 20 photons detected which correspond to 6.1 G-band magnitude fast transient. For even faster limit, we get limiting fluence of  $\sim 133$  photons per square meter within 100ns. The crosstalk is higher than expected, possibly due to reflection in system design or defect in SiPMs. Also, the spatial resolution of the system is expected to be improved to 10 arcseconds level for more dedicated scientific measurements. Further developments and field testings will be performed in the Ultra Fast Astronomy program to explore the high time resolution domain of astrophysics.

## Appendix A: SiPM models spectral response

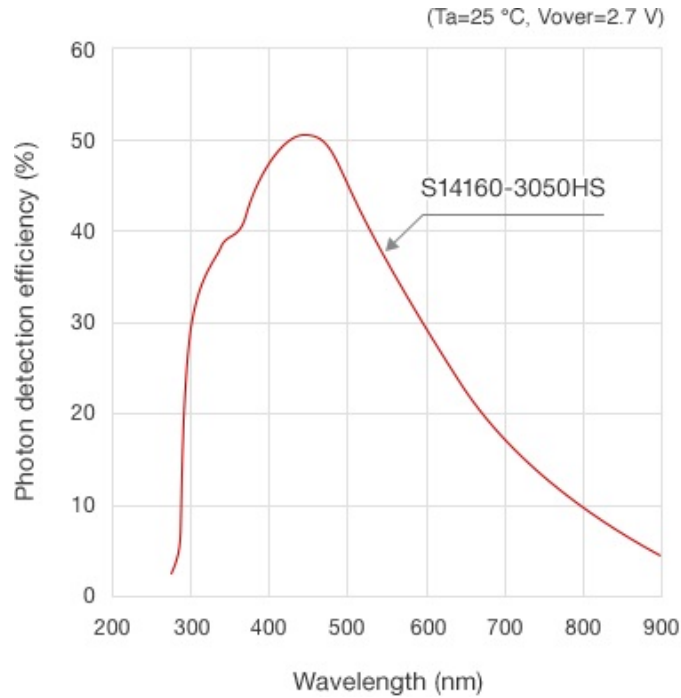


Fig 12: Hamamatsu SiPM S14160-3050HS spectral response curve

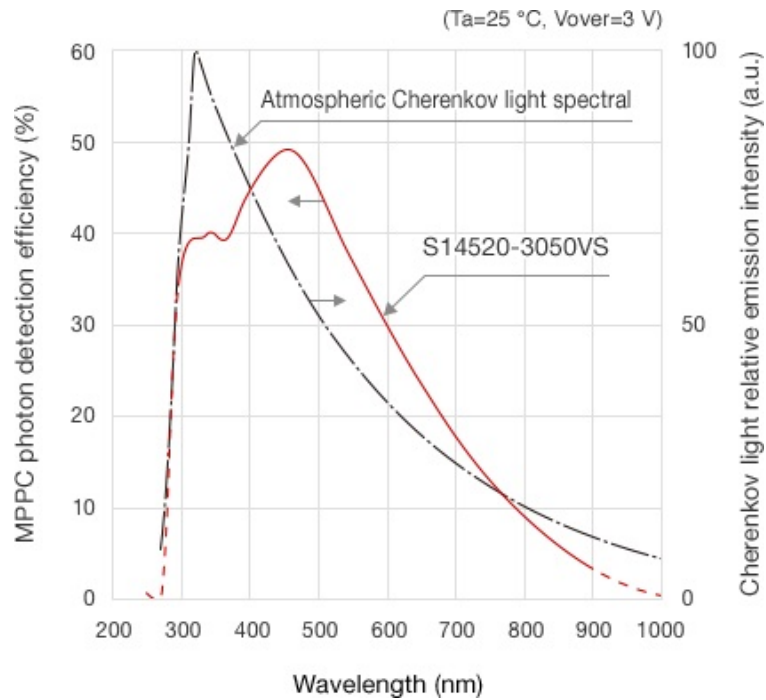


Fig 13: Hamamatsu SiPM S14520-3050VS spectral response curve

Credit to Hamamatsu photonics

## Appendix B: SiPM units breakdown voltage versus temperature calibration curves, tested in laboratory condition

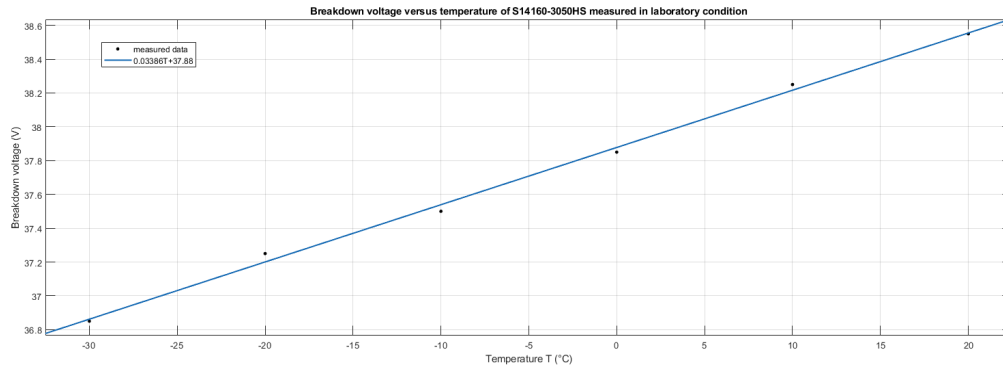


Fig 14: Hamamatsu SiPM S14160-3050HS breakdown voltage versus temperature calibration curve

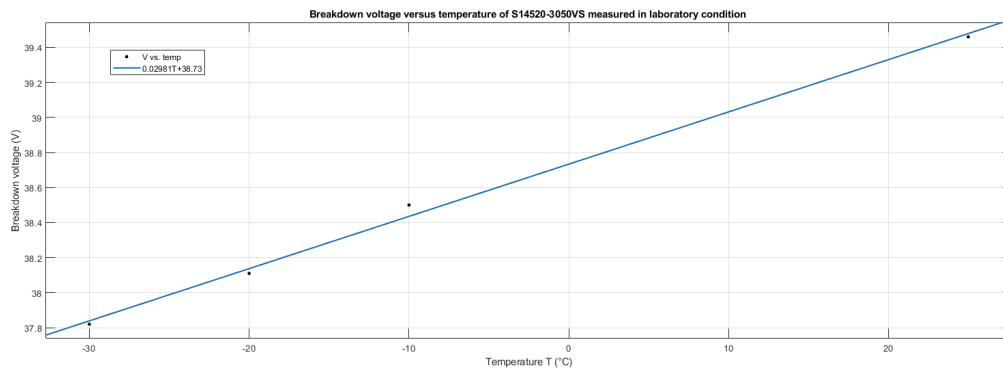


Fig 15: Hamamatsu SiPM S14520-3050VS breakdown voltage versus temperature calibration curve

## Appendix C: Analysed Data from S14160-3050HS

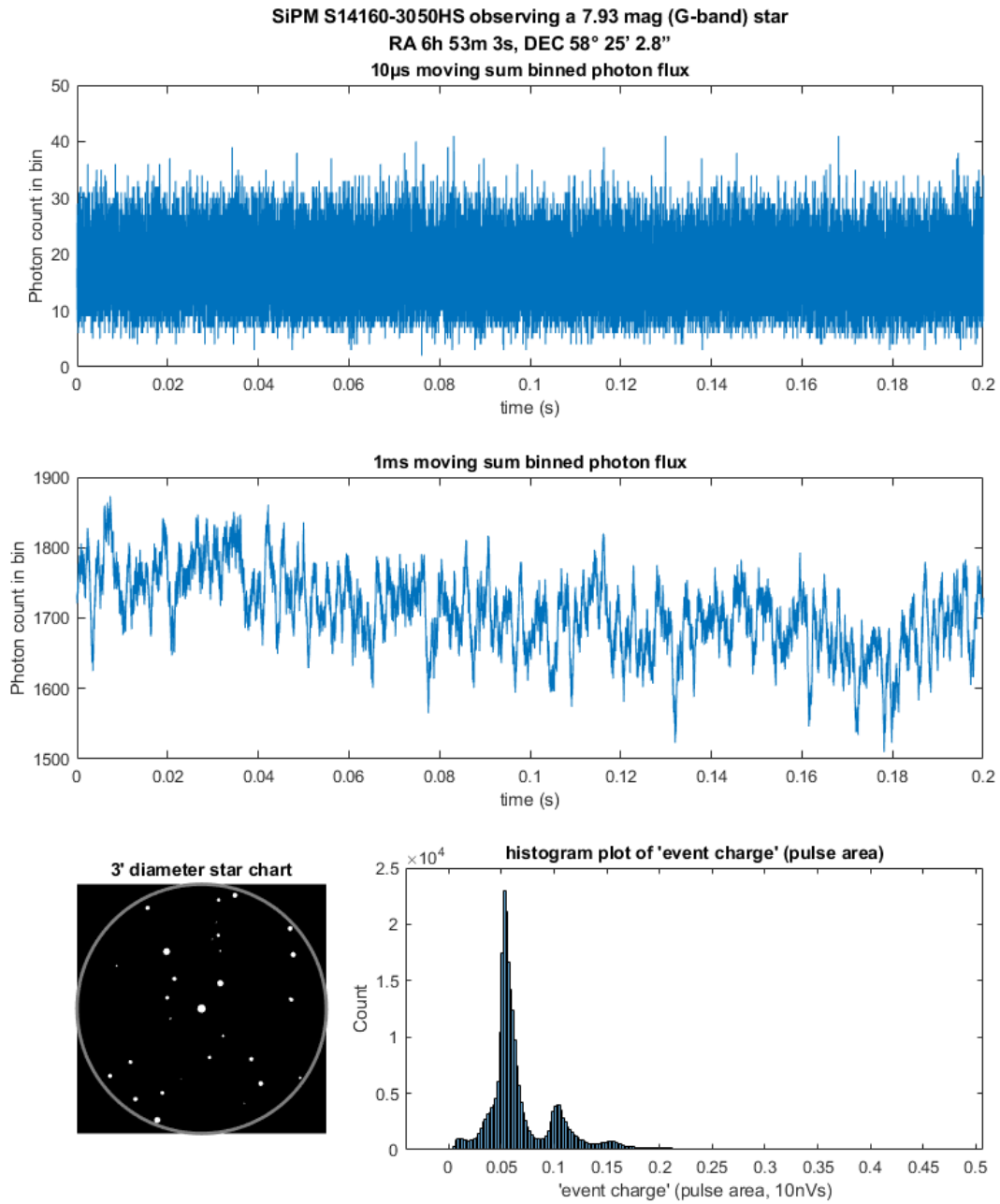


Fig 16: SiPM S14160-3050HS observing HIP32890

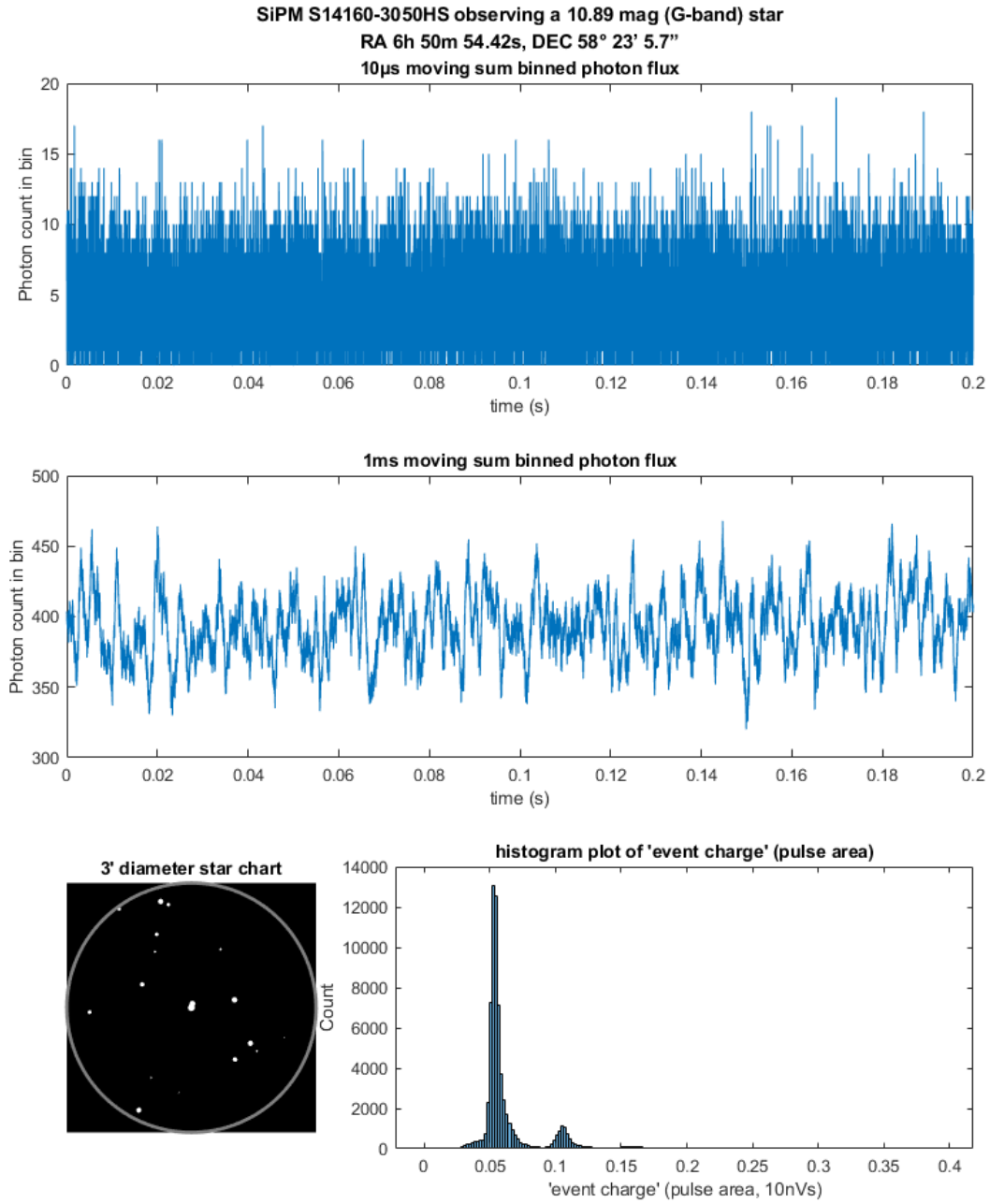


Fig 17: SiPM S14160-3050HS observing a 10.89 mag (G-band) star

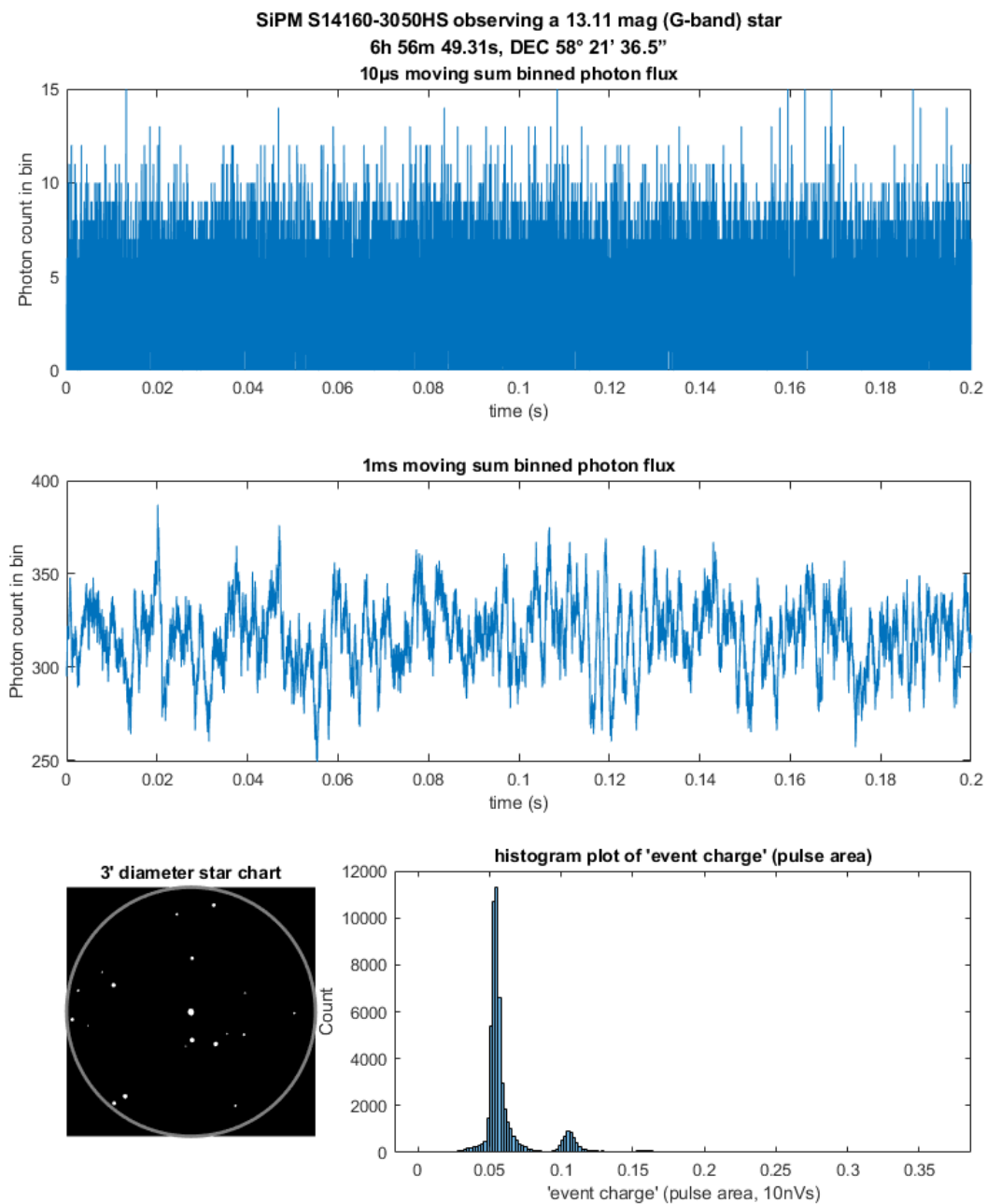


Fig 18: SiPM S14160-3050HS observing a 13.11 mag (G-band) star

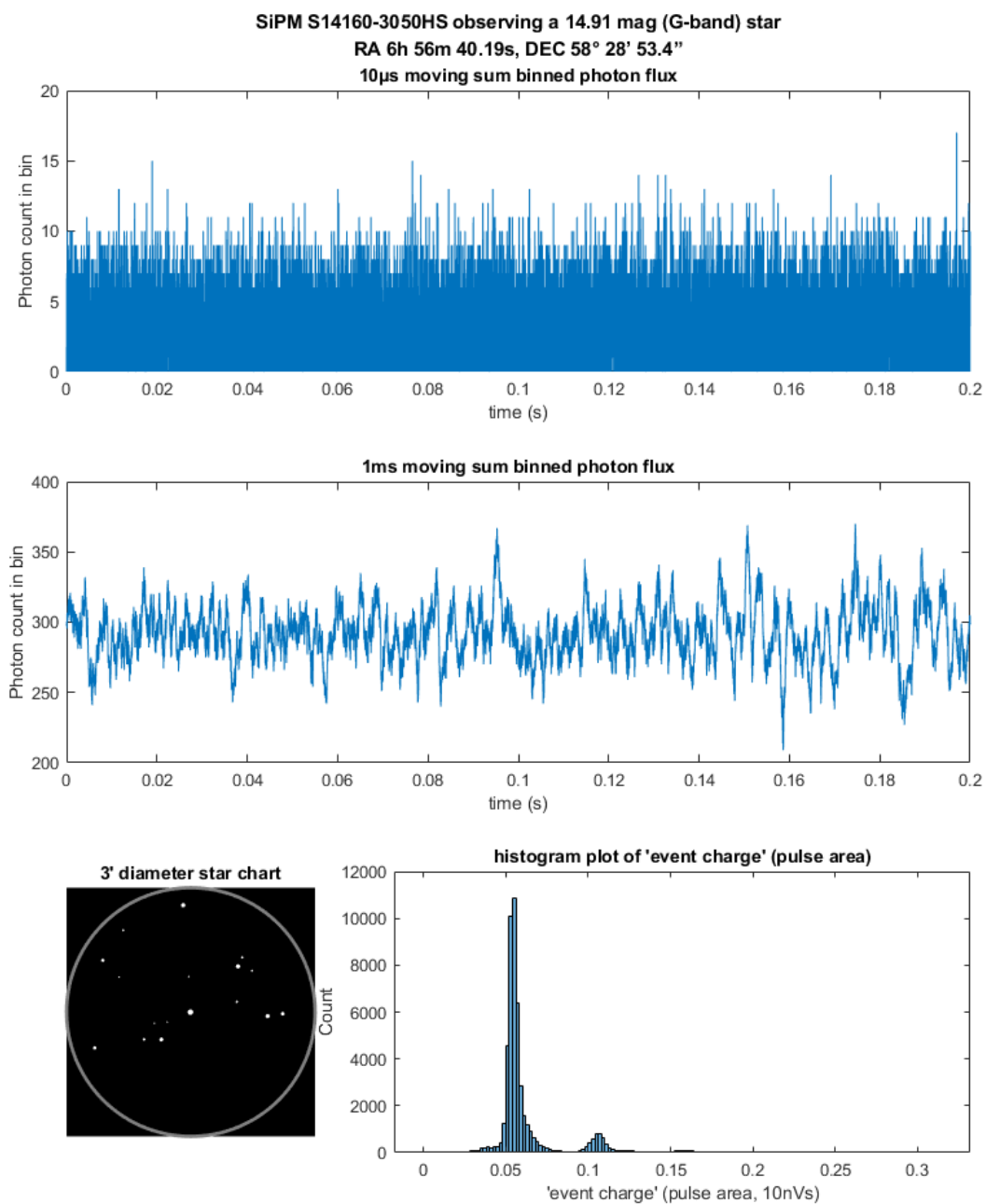


Fig 19: SiPM S14160-3050HS observing a 14.91 mag (G-band) star



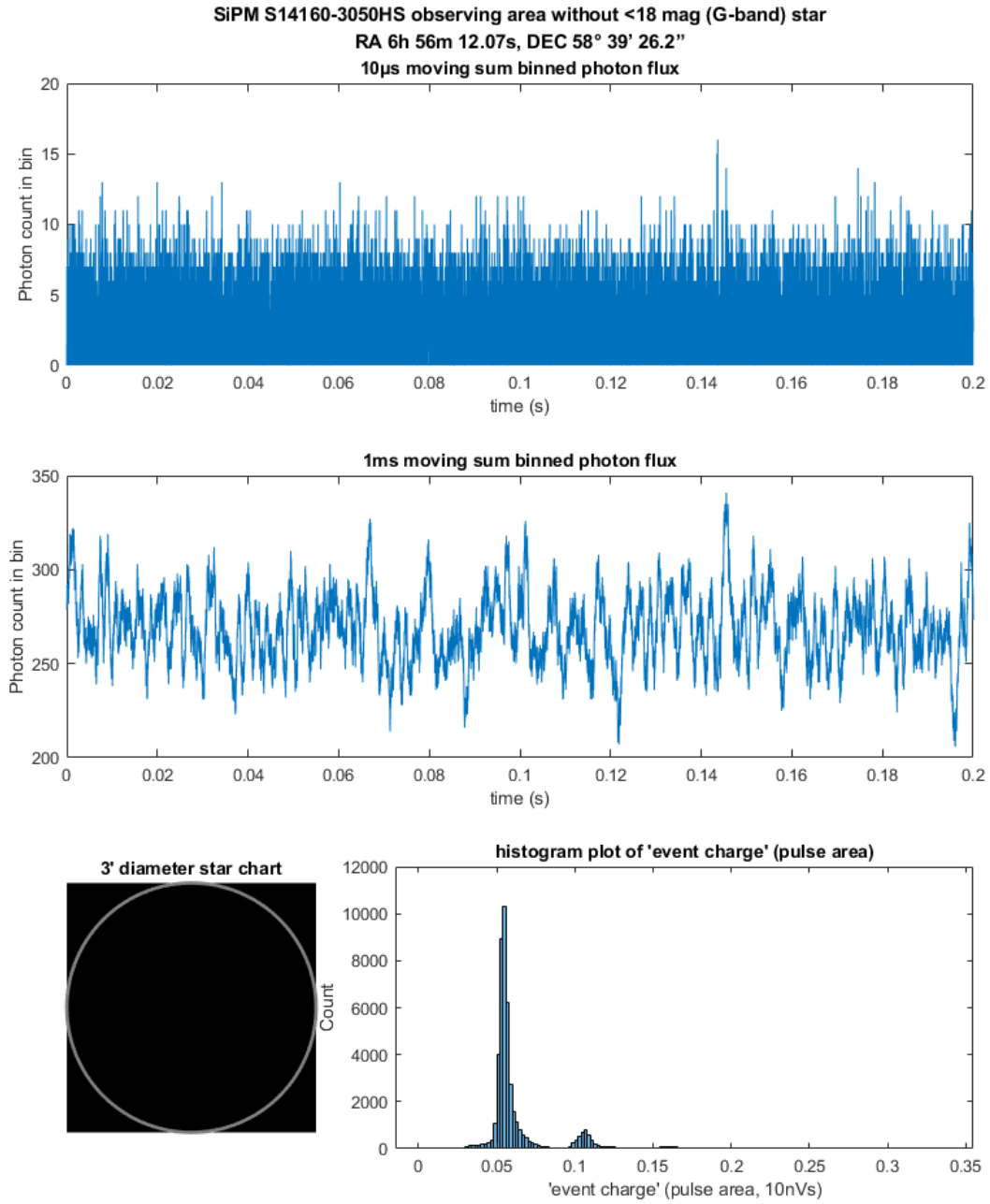


Fig 20: SiPM S14160-3050HS observing area without star brighter than 18 mag (G-band)

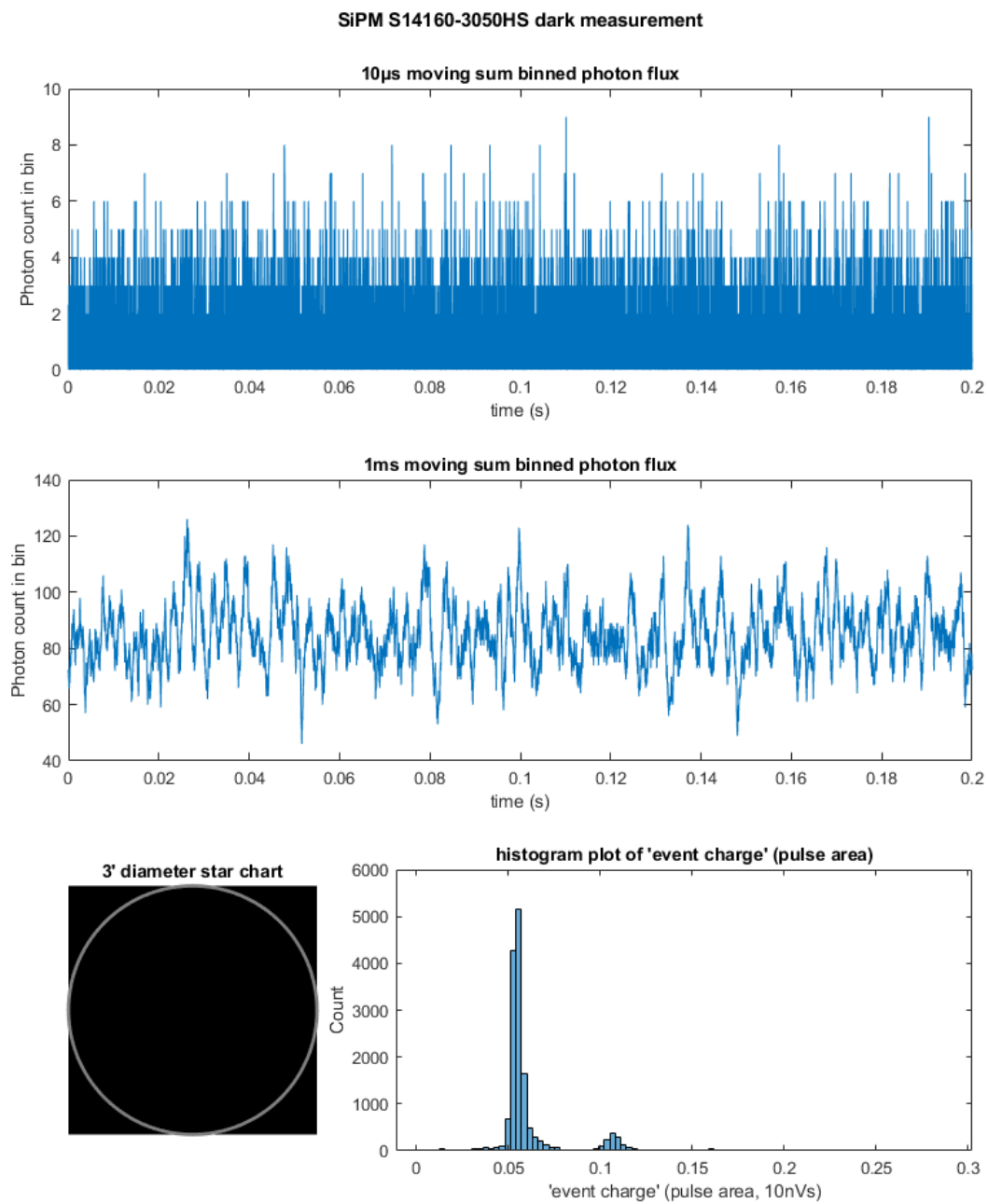


Fig 21: SiPM S14160-3050HS dark measurement on site

## Appendix D: Analysed Data from S14520-3050VS

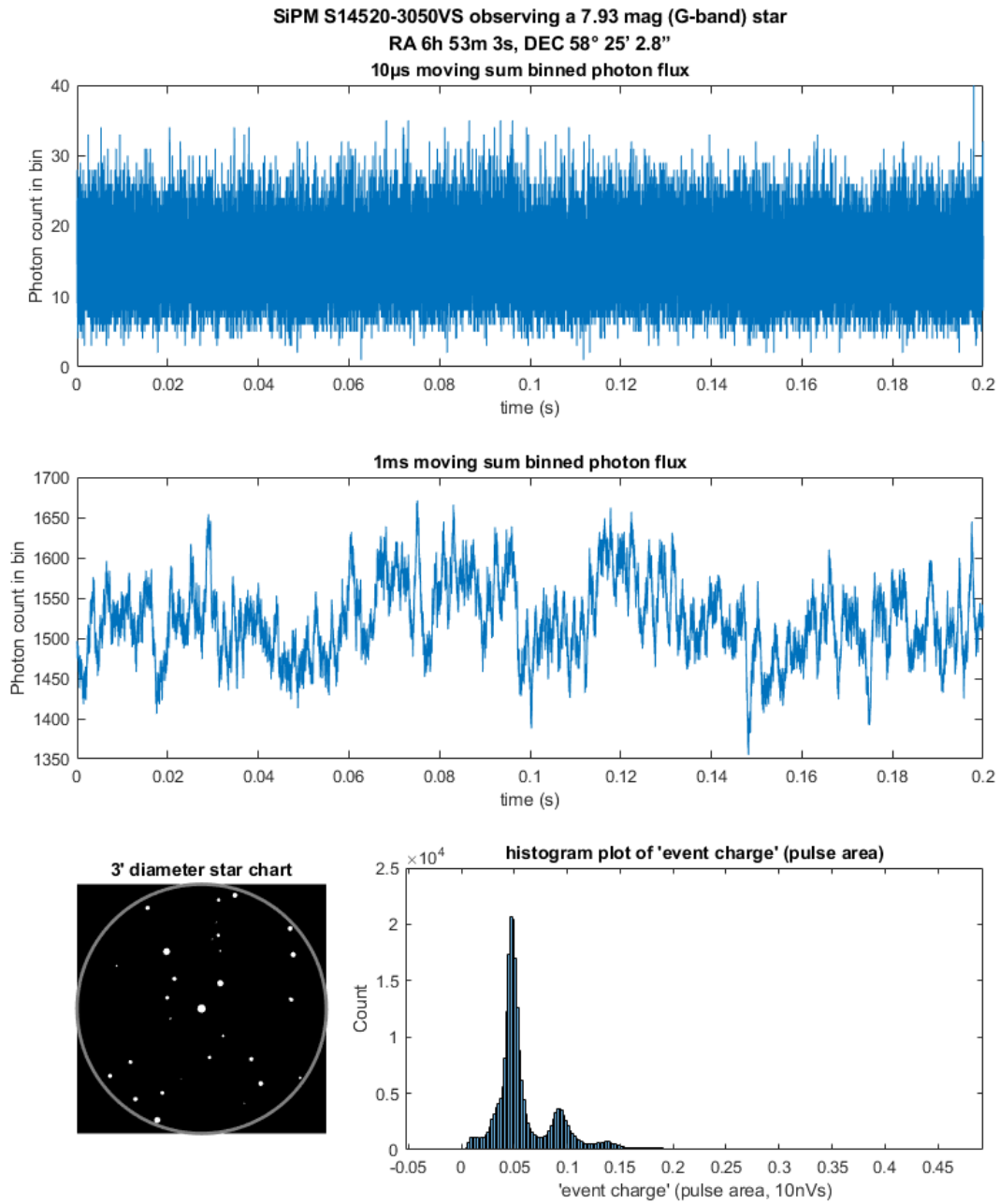


Fig 22: SiPM S14520-3050HS observing HIP32890

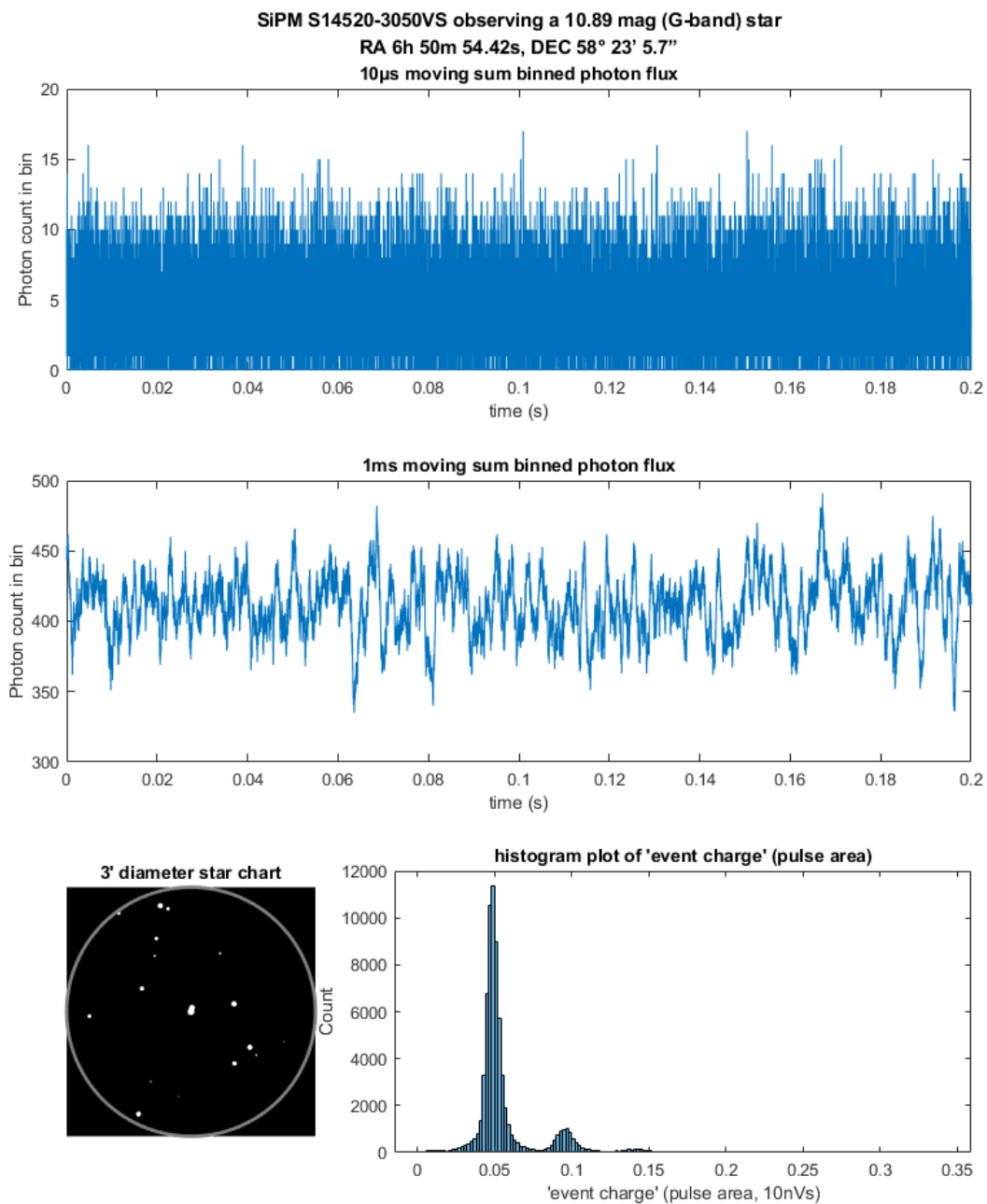


Fig 23: SiPM S14520-3050HS observing a 10.89 mag (G-band) star

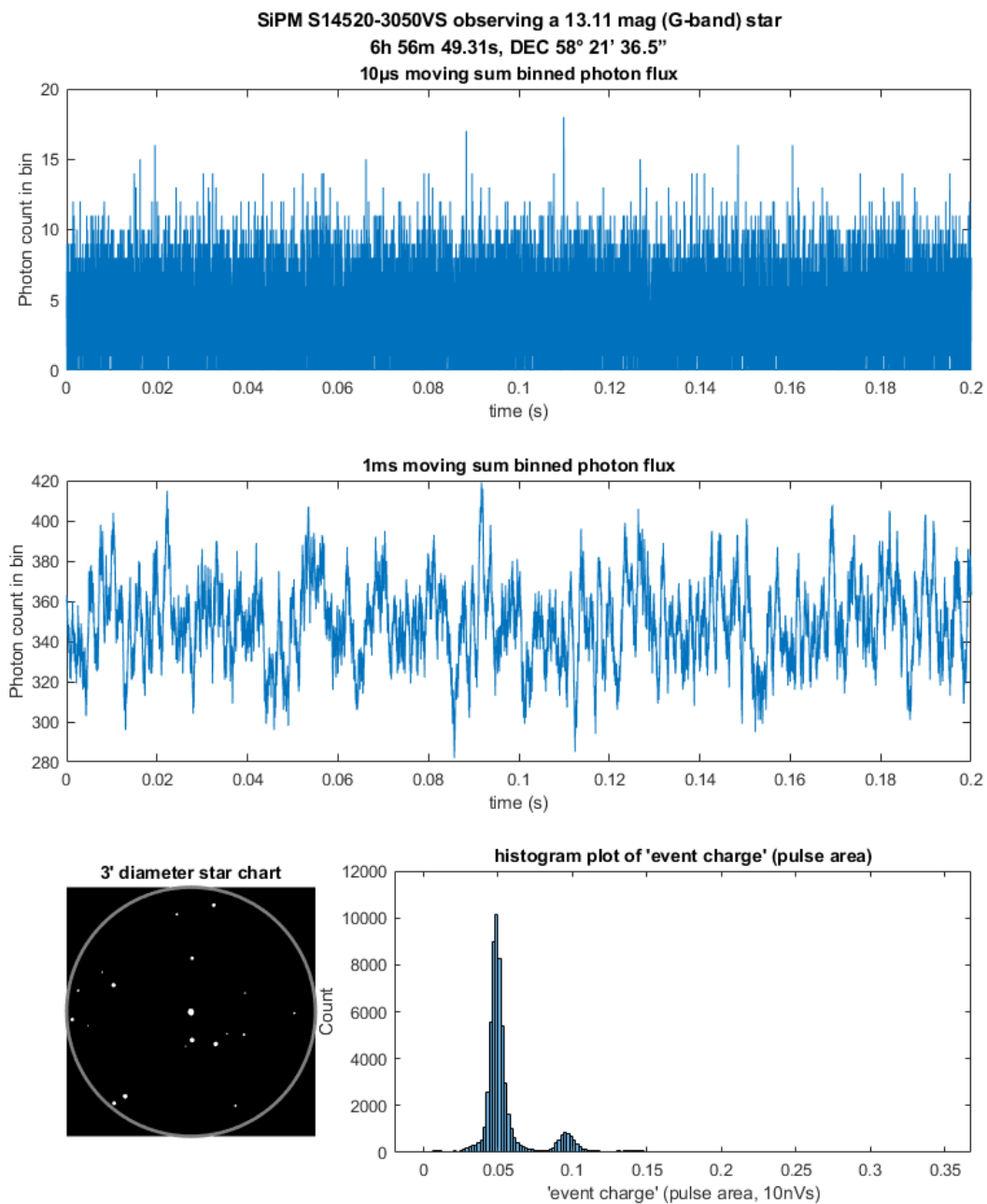


Fig 24: SiPM S14520-3050HS observing a 13.11 mag (G-band) star

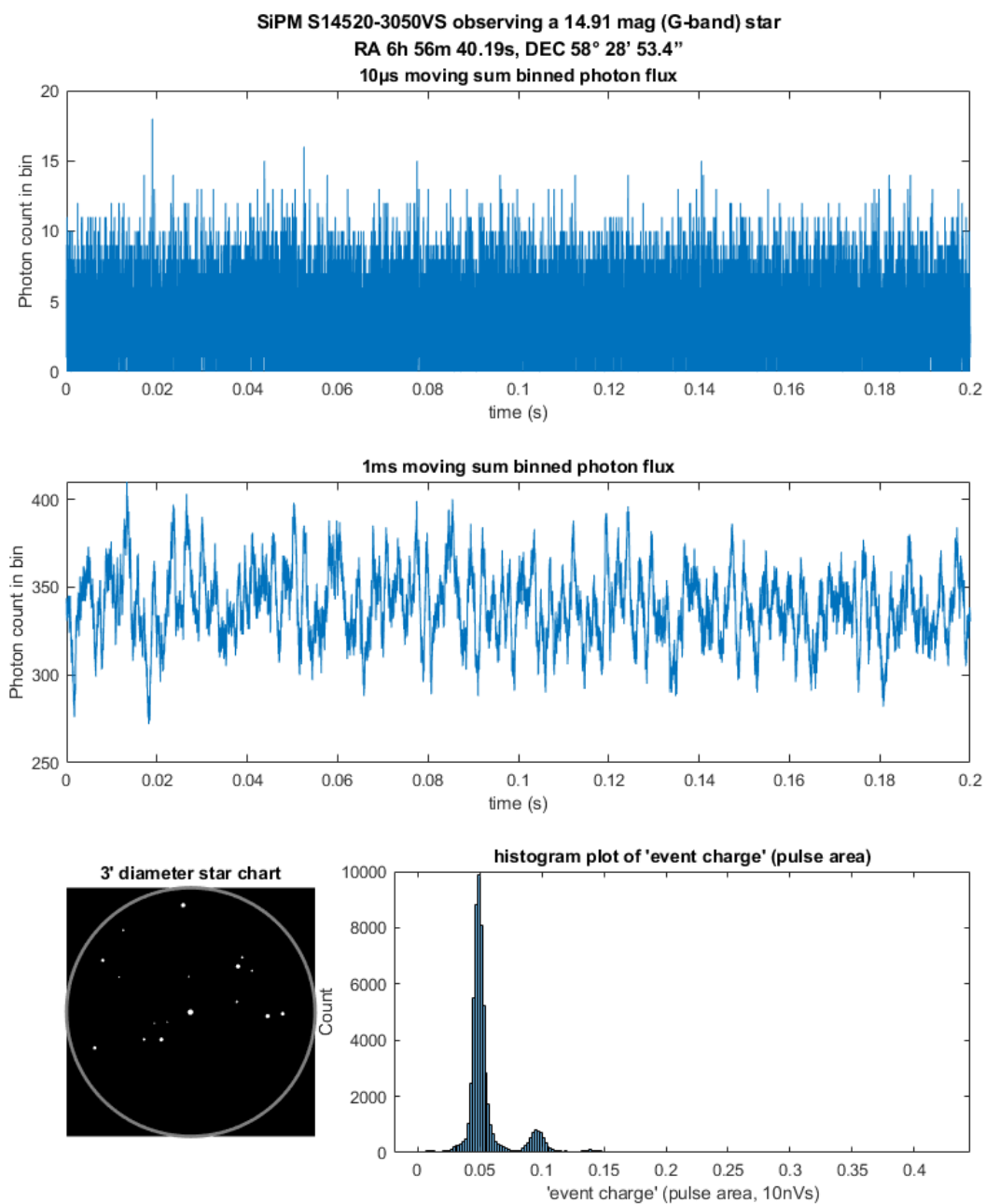


Fig 25: SiPM S14520-3050HS observing a 14.91 mag (G-band) star

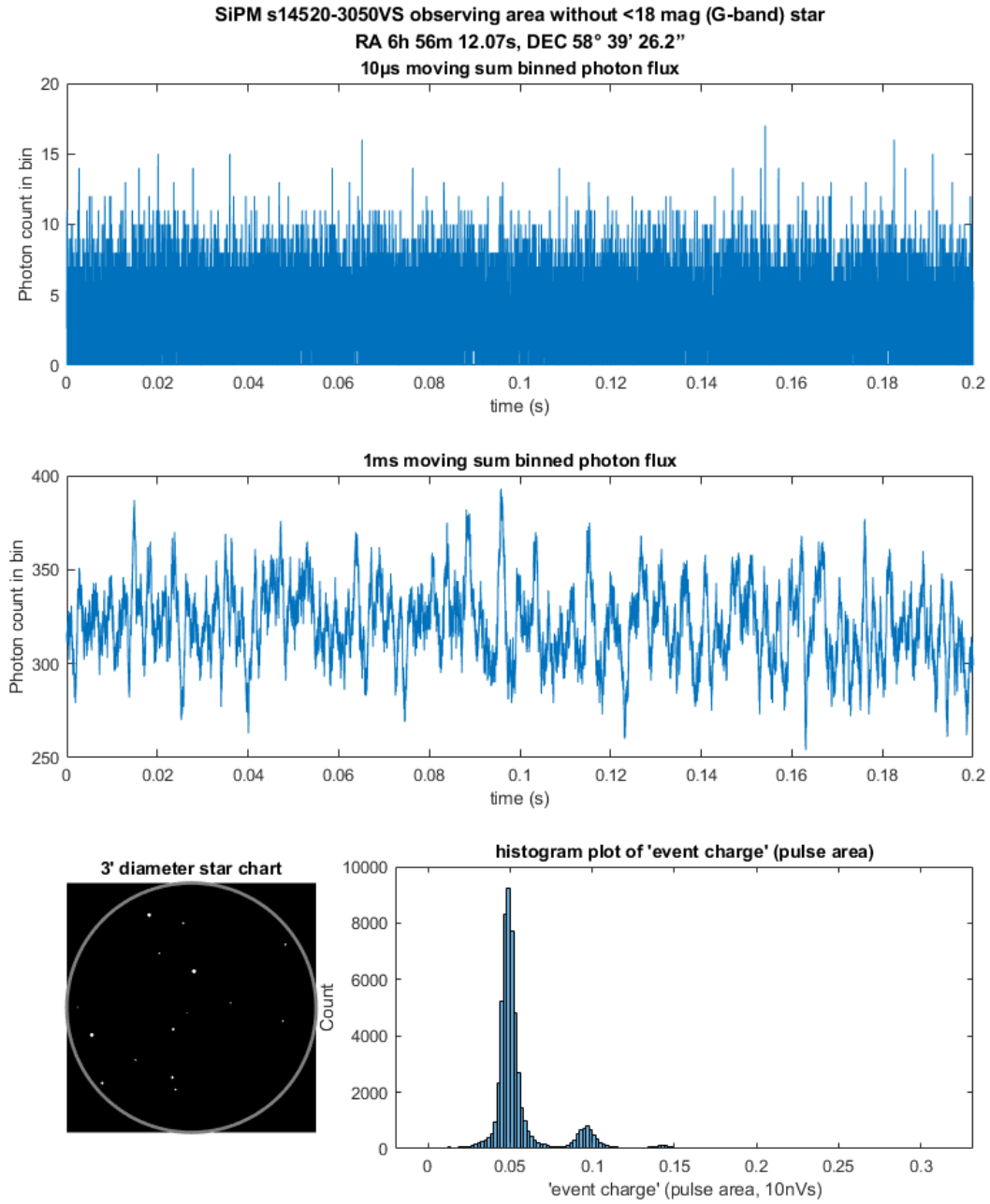


Fig 26: SiPM S14520-3050HS observing area without star brighter than 18 mag (G-band)

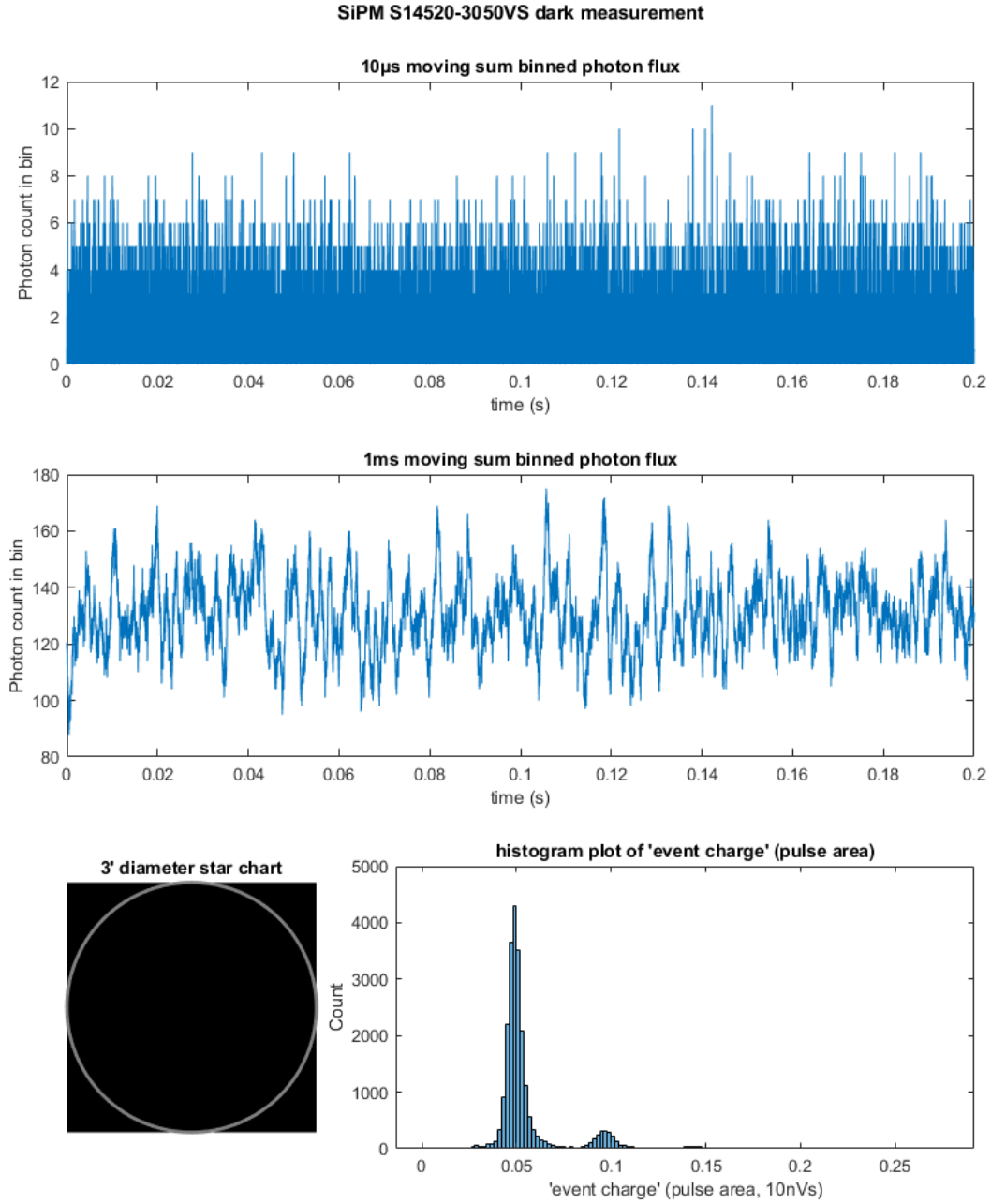


Fig 27: SiPM S14520-3050HS dark measurement on site

### *Acknowledgments*

We would like to thank support from RK MES grant AP05135753 through Nazarbayev University, Kazakhstan. We would also like to thank support from HKUST Jockey Club Institute for Advanced



Study (IAS).

We would like to offer special thanks to research and support team, especially engineer Maxim Krugov at the Assy Turgan Observatory, Fesenkov Astrophysical Institute for their support, help and advice during the experiment.

We wish to acknowledge the help on preparing the experiment by technicians in Physics Departments of HKUST, Ulf Lampe and TK Cheng.

This work has made use of data from Hamamatsu photonics.

This work has made use of data from the European Space Agency (ESA) mission *Gaia* (<https://www.cosmos.esa.int/gaia>), processed by the *Gaia* Data Processing and Analysis Consortium (DPAC, <https://www.cosmos.esa.int/web/gaia/dpac/consortium>). Funding for the DPAC has been provided by national institutions, in particular the institutions participating in the *Gaia* Multilateral Agreement.

## References

- 1 S. Li, G. F. Smoot, B. Grossan, *et al.*, “Program objectives and specifications for the Ultra-Fast Astronomy observatory,” in *AOPC 2019: Space Optics, Telescopes, and Instrumentation*, S. Xue, X. Zhang, C. A. Nardell, *et al.*, Eds., **11341**, 513 – 521, International Society for Optics and Photonics, SPIE (2019).
- 2 L. K. Hardy, V. S. Dhillon, L. G. Spitler, *et al.*, “A search for optical bursts from the repeating fast radio burst frb 121102,” *Monthly Notices of the Royal Astronomical Society* **472**(3), 2800–2807 (2017).
- 3 M. Cosens, J. Maire, S. A. Wright, *et al.*, “Panoramic optical and near-infrared seti instru-

- ment: prototype design and testing,” in *Ground-based and Airborne Instrumentation for Astronomy VII*, **10702**, 107025H, International Society for Optics and Photonics (2018).
- 4 B. Grossan, P. Kumar, and G. F. Smoot, “The emission mechanism of gamma-ray bursts: Identification via optical-ir slope measurements,” *Journal of High Energy Astrophysics* **23**, 14–22 (2019).
  - 5 G. Collaboration *et al.*, “Description of the gaia mission (spacecraft, instruments, survey and measurement principles, and operations),” *Gaia Collaboration et al.(2016a): Summary description of Gaia DRI* (2016).
  - 6 G. Collaboration *et al.*, “Summary of the contents and survey properties,” *arXiv preprint arXiv:1804.09365* (2018).
  - 7 V. Saveliev, “The recent development and study of silicon photomultiplier,” *Nuclear Instruments and Methods in Physics Research Section A: Accelerators, Spectrometers, Detectors and Associated Equipment* **535**(1-2), 528–532 (2004).
  - 8 K. Yamamoto, T. Nagano, R. Yamada, *et al.*, “Recent development of mppc at hamamatsu for photon counting applications,” in *Proceedings of the 5th International Workshop on New Photon-Detectors (PD18)*, 011001 (2019).
  - 9 HP *Low Noise, Cascadable Silicon Bipolar MMIC Amplifier* (N.D.).
  - 10 Tektronix, “Always-on power,” (N.D.).
  - 11 G. J. McLachlan and D. Peel, *Finite mixture models*, John Wiley & Sons (2004).
  - 12 G. McLachlan, “Peel., d,” *Finite Mixture Models* (2000).
  - 13 D. Arthur and S. Vassilvitskii, “k-means++: The advantages of careful seeding,” in *Proceed-*

ings of the *eighteenth annual ACM-SIAM symposium on Discrete algorithms*, 1027–1035, Society for Industrial and Applied Mathematics (2007).

- 14 F. Kasten and A. T. Young, “Revised optical air mass tables and approximation formula,” *Applied optics* **28**(22), 4735–4738 (1989).
- 15 A. Kinkhabwala and S. Thorsett, “Multifrequency observations of giant radio pulses from the millisecond pulsar b1937+ 21,” *The Astrophysical Journal* **535**(1), 365 (2000).

Biographies of the authors are not available.

## List of Figures

- 1 Experimental Setup for UFA project. The left image shows the telescope on whose right side is the port on which the SiPM experiment is mounted. The center shows the SiPM mount, hardware and electronics and on the right an image of the oscilloscope used to take the observations.
- 2 (Top) dark count raw data which was measured by S14520-3050VS, (bottom) processed data after filtration and baseline cancellation.
- 3 A histogram plot of pulse area of different photon pulses. Notice the first and second peaks are both Gaussian like and hence we use the Gaussian Mixture model for fitting.
- 4 Part of data saturated by photon flux from 14 Lyn using SiPM S14520-3050VS.
- 5 histogram plot from the above saturated data.
- 6 SiPM Count in 0.2s versus calibrated G-band flux for s14160-3050HS
- 7 Measured crosstalk versus count rate for s14160-3050HS

- 8 Count rate versus calibrated G-band flux for S14520-3050VS.
- 9 Measured crosstalk versus count rate for S14520-3050VS.
- 10  $10\mu s$  (top) and 1ms (bottom) smoothed signal from synthetic 100Hz scattered square wave light.
- 11 Poisson statistical fitting of SiPM measurement on a sample dark sky
- 12 Hamamatsu SiPM S14160-3050HS spectral response curve
- 13 Hamamatsu SiPM S14520-3050VS spectral response curve
- 14 Hamamatsu SiPM S14160-3050HS breakdown voltage versus temperature calibration curve
- 15 Hamamatsu SiPM S14520-3050VS breakdown voltage versus temperature calibration curve
- 16 SiPM S14160-3050HS observing HIP32890
- 17 SiPM S14160-3050HS observing a 10.89 mag (G-band) star
- 18 SiPM S14160-3050HS observing a 13.11 mag (G-band) star
- 19 SiPM S14160-3050HS observing a 14.91 mag (G-band) star
- 20 SiPM S14160-3050HS observing area without star brighter than 18 mag (G-band)
- 21 SiPM S14160-3050HS dark measurement on site
- 22 SiPM S14520-3050HS observing HIP32890
- 23 SiPM S14520-3050HS observing a 10.89 mag (G-band) star
- 24 SiPM S14520-3050HS observing a 13.11 mag (G-band) star
- 25 SiPM S14520-3050HS observing a 14.91 mag (G-band) star
- 26 SiPM S14520-3050HS observing area without star brighter than 18 mag (G-band)
- 27 SiPM S14520-3050HS dark measurement on site

## List of Tables

- 1 Specification of the SiPMs
- 2 Specification of telescope NUTTelA-TAO (CDK700)
- 3 Observation log for 28/10/2019
- 4 Observation log for 29/10/2019
- 5 Measured data from S14160-3050HS
- 6 Measured data from S14520-3050VS